Journal of Glaciology, Vol. 40, No. 135, 1994

The character, structure and origin of the basal ice layer of a surge-type glacier

MARTIN SHARP*,
Department of Geography, University of Cambridge, Cambridge CB2 3EN, England

JEAN JOUZEL,
Service de Physique et de Physico-Chimie, Laboratoire de Géochimie Isotopique, Centre d'Études Nucléaires de Saclay, F-91191 Gif-sur-Yvette Cedex, France

BRYN HUBBARD,
Department of Geography, University of Cambridge, Cambridge CB2 3EN, England

WENDY LAWSON
Department of Geography, University of Auckland, Auckland, New Zealand

ABSTRACT. The basal ice layer of surge-type Variegated Glacier, Alaska, appears to have formed by a combination of (i) open-system freezing of subglacial meltwaters over both rigid and unconsolidated substrates; (ii) apron over-riding during surge-induced glacier advance; (iii) incorporation of glacier ice by recumbent folding, thrust-faulting and nappe over-riding during down-glacier propagation of a surge front; and (iv) post-formational metamorphism involving recrystallization, partial internal melting and squeezing out of meltwaters and dissolved gases. Structural evidence and the characteristics of debris entrained in ice facies formed by basal freezing suggest that the layer includes a lower element formed under surge conditions and an upper element formed during the quiescent phase of a surge cycle. The lower element is depleted in comminution products and enriched in medium gravel, while the upper element contains comminution products but virtually no medium gravel. This distinction is attributed to the efficiency of bedrock fracture and meltwater flushing of comminution products under surge conditions. The basal ice layer thickens from <1 m to >13 m down-glacier in a manner consistent with the magnitude of horizontal shortening induced by the 1982–83 surge. Thickening is largely tectonic in origin, and the style and intensity of folding and thrust faulting change down-glacier as the magnitude of horizontal shortening increases. Tectonic processes associated with the down-glacier propagation of surge fronts therefore appear to be capable of creating thick basal ice layers which allow extensive supraglacial sedimentation of subglacially derived debris.

INTRODUCTION

In this paper we present the results of an investigation into the origin of the basal ice layer of Variegated Glacier, Alaska, one of the world's most intensively studied surge-type glaciers (Raymond, 1987). The objectives of the study are: (i) to describe and establish the genesis of the various ice facies which comprise the basal ice layer; (ii) to link the formation of the basal ice layer to the glacier's surge cycle; (iii) to analyse the structure and stratigraphy of the basal ice layer in order to evaluate the relative importance of primary entrainment processes and subsequent tectonic deformation as influences on its geometry; and (iv) to evaluate the geomorphological implications of the inferred origin of the basal ice layer. The work is significant because there have been no previous descriptions of the basal ice layers of surge-type glaciers, even though the ability of such glaciers to form unusually thick basal ice layers may result in them having distinctive geomorphological effects which should be recognizable in the stratigraphical record (Clapperton, 1975; Sharp, 1985a, b, 1988).

GEOGRAPHICAL SETTING

Variegated Glacier is a 20 km long surge-type glacier, located on the southern side of the St Elias mountains in southeastern Alaska, about 55 km north of Yakutat. From

* Present Address: Department of Geography, University of Alberta, Edmonton, Alberta T6G 2H4, Canada.

https://doi.org/10.3189/S0022143000007413 Published online by Cambridge University Press

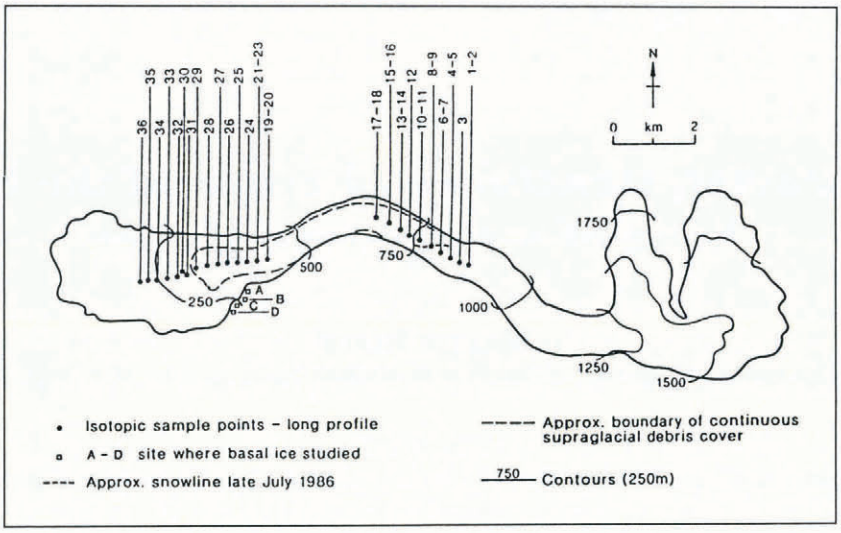

Fig. 1. Map of Variegated Glacier, Alaska, showing the location of the long profile along which snow and Ed-facies ice were sampled and of sites A–D, where basal ice was investigated.

wide accumulation basins at elevations of up to 1950 m on the Alaska–Yukon border, it flows westward into a narrow, steep-sided, meandering valley before eventually terminating in a broad lobe of stagnant, debris-covered ice on the shores of Russell Fjord (Fig. 1). The valley cuts through fault-shattered intrusive and medium-grade metamorphic rocks (Frost, 1976). The main lithologies exposed in the valley walls include ortho-amphibolite, ortho- and para-gneiss and pelitic schist. The glacier has a temperate thermal regime (Bindschadler and others, 1976); its geometry has been described by Bindschadler and others (1977).

Variegated Glacier has a well-documented history of surging, five surges having occurred since 1905–06 at an average interval of 18–20 years (Tarr and Martin, 1914; Post, 1969; Bindschadler and others, 1977; Kamb and others, 1985). The most recent of these occurred in 1982–83, 3 years before the field work for this study was carried out. The evolution of the geometry and flow dynamics of the glacier prior to this surge has been discussed by Raymond and Harrison (1988), while the details of the surge itself have been described in a number of papers (Kamb and others, 1985; Kamb, 1987; Raymond, 1987; Raymond and others, 1987). Of particular relevance to the present study are descriptions of tectonic processes, structural evolution and the deformation history of the glacier (Raymond and others, 1987; Sharp and others, 1988; Pfeffer, 1992; Lawson and others, in press).

The basal ice layer described in this study is exposed in four sections located along the southern latero-frontal margin of the glacier (Fig. 1). These are labelled A–D with increasing distance down-glacier, and they lie within the area affected by intense longitudinal compression and tectonic thickening during propagation of the 1982–83 surge front into the stagnant ice of the terminal lobe (Raymond and others, 1987; Sharp and others, 1988). The thickness of the basal ice layer therefore increases from a few decimetres at site A to over 13 m at site D. Sites A–C, which are located along the lateral margin of the glacier, experienced limited glacier advance from the north (i.e. perpendicular to the normal flow direction) in association with the 75 m of thickening which occurred as ice was re-activated by down-glacier propagation of the surge front. Site D is adjacent to the outlet of one of the two principal meltwater streams draining the glacier. The glacier advanced over the outwash deposited by this stream during the 1983 summer, re-activating dead ice buried beneath outwash gravels in the process. C. F. Raymond obtained a time-lapse photographic record of the advance of the glacier in this area with a Super-8 camera.

Table 1. Summary of the debris content and electrical conductivity characteristics of those ice facies observed at Variegated Glacier for which data are available

Facies	*Mean debris content*	*Std dev.*	*Mean debris content*	*Std dev.*	*Mean electrical conductivity*	*Std dev.*
	g l^{-1}		vol. %		μS cm^{-1}	
Englacial facies						
Englacial diffused	8.6	10.0	0.3	0.4	26.6	8.8
Snow					9.7	0.8
Basal facies						
Basal diffused	3.4	2.9	0.1	0.1	21.2	7.5
Basal stratified laminated	417.8	480.0	10.9	15.1	44.0	15.7
Basal stratified clear	10.5	5.6	0.4	0.2	22.8	5.7
Basal stratified solid	1496.4	1857.8	35.7	40.8	60.7	8.1

ANALYTICAL METHODS

Types of ice observed at Variegated Glacier were classified into facies using the following criteria: ice-crystal size, air-bubble content and distribution, concentration and mode of dispersion of debris within the ice, electrical conductivity of the melted ice and the thickness and geometry of individual ice units (Table 1) (cf. Lawson, 1979). Samples of debris for textural analysis were collected from those facies which had outcrops sufficiently extensive or debris concentrations high enough to make such sampling meaningful. Ice blocks, the size of which was inversely proportional to the apparent debris concentration, were cut from exposures from which weathered surface ice had previously been removed using an ice hammer. These blocks were placed in large polythene bags and allowed to melt. The water–sediment mix was repeatedly filtered through Whatman 542 hardened ashless filter papers, using the filtrate to wash the polythene bag between each filtration step. Volume of filtrate and weight of entrapped sediment after ashing at 550°C were recorded for calculation of debris concentrations. Grain-size distributions were determined by dry sieving at 1Φ intervals between –5 and 3Φ and by laser granulometry between 3 and 9Φ.

The resulting grain-size distributions were invariably polymodal, so the technique of Gaussian component analysis (Sheridan and others, 1987) was used to deconvolute each grain-size distribution into its constituent sub-populations. The mean size and standard deviation of each sub-population were calculated, together with the fraction of the total sample which fell into each sub-population and the magnitude of the unexplained residuum. Three or four Gaussians were required to describe the samples collected, leaving unexplained residua of 3.5–14%. Each of these populations should be interpretable in terms of processes of comminution, selective entrainment or deposition which affect debris during transport through the glacier (Haldorsen, 1981).

To facilitate interpretation of the genesis of the ice facies, their composition in δD and δ^{18}O was determined. The technique of co-isotopic analysis has the potential to discriminate between glacier ice and ice formed by the refreezing of meltwater, to determine the character of the hydrological environment in which freezing took place and to identify the source of water involved (Jouzel and Souchez, 1982; Souchez and Jouzel, 1984). Hence, samples of both englacial and basal facies were collected. To obtain an idea of the range of isotopic compositions characteristic of englacial facies and snowfall in the area, ice samples were collected along a transect up the centre line of the glacier (Fig. 1). Basal facies were sampled at sites B–D. Sampling was carried out as follows: weathered surface ice was first removed with an ice hammer to a depth of at least 20 cm. Samples were retrieved with a 2.4 cm external diameter aluminium ice screw and stored in the shade in sealed polythene bottles while they melted. Immediately after melting, samples were press-filtered into dark-glass vials which were completely filled and sealed with Parafilm. These vials were stored in a dark box and, after return from the field, in a refrigerator at 4°C before transfer to the laboratory for analysis. Samples were analysed at the Centre d'Études Nucléaires de Saclay by twin mass spectrometers, allowing co-isotopic measurements on a single liquid drop. δD and δ^{18}O values are expressed in ppt (‰) relative to Vienna standard mean ocean water (SMOW). Accuracy of the measurements is 0.5‰ for δD and 0.15‰ for δ^{18}O. The accuracy in δ^{18}O places some limitations on the extent to which *quantitative* interpretation of the data is possible.

CHARACTERISTICS OF THE ICE FACIES AND INCLUDED DEBRIS

In classifying facies, we made a primary distinction between *englacial* facies ice, composed of relatively homogeneous foliated glacier ice, and *basal stratified* facies ice (Table 1). The latter usually underlay the englacial facies and was distinguished by its generally higher debris content and more variable ice characteristics (Fig. 2). In recognition of this variability, the basal stratified facies was subdivided into three sub-facies. We also recognized a *basal diffused* facies, which cropped out within the basal ice layer but had physical characteristics similar to those of the englacial facies.

Fig. 2. Basal ice layer at site D, showing the breccia of blocks of Bd-facies ice at the base of the sequence, and the sharp boundary between the englacial diffused and basal stratified facies. The shelf marking this boundary occurs approximately 13 m above the bed.

Englacial diffused facies (Ed)

This facies comprised the bulk of the glacier and consisted of strongly bubble-foliated, debris-poor ice, with occasional thin layers of clear, blue ice and fine-grained ice. Ice crystals reached 8 cm in diameter. Debris occurred as dispersed aggregates which were sometimes concentrated along poorly defined planes sub-parallel to the bubble foliation. Debris concentrations averaged 0.3% by volume. Electrical conductivities averaged 26.6 μS cm^{-1}, somewhat higher than values measured on overlying snow (mean 9.7 μS cm^{-1}) (Table 1). This difference can be explained in terms of the greater leaching by

https://doi.org/10.3189/S0022143000007413 Published online by Cambridge University Press

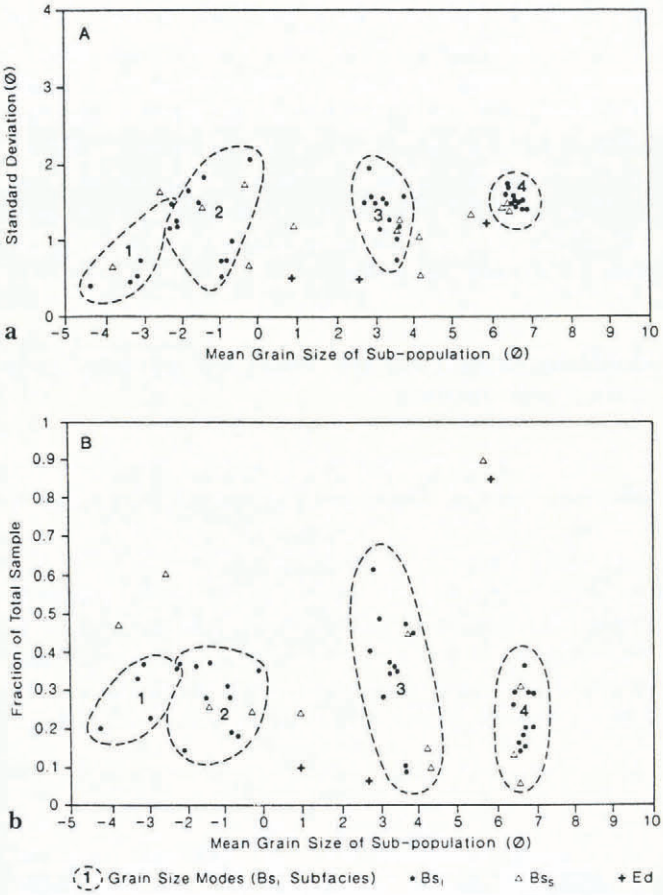

Fig. 3. Results of Gaussian component analysis of particle-size distributions of samples of debris collected from ice facies at Variegated Glacier: a. Standard deviation versus mean size for each component recognized; b. Proportion of the sample falling into each component as a function of the mean size for that component.

percolating meltwater from snow deposited within the ablation zone of the glacier than from snow deposited at higher elevations (the presumed origin of glacier ice). Debris consisted primarily of coarse to medium silt ($5.81 \pm 1.19\Phi$; 84%), with additional minor modes in the coarse (10%) and fine (6%) sand-size ranges (Fig. 3). The combined evidence of fine mean grain-size, high degree of sorting and the dispersed distribution of the debris in the ice suggests an aeolian origin for the primary mode. The coarse-sand mode included angular lithic fragments which were presumably derived from the valley walls. The absence of coarser material of similar provenance in samples from this facies can be explained in terms of the relatively small size of ice sample collected for analysis.

Englacial banded facies (Eb)

This facies consisted of debris-rich layers of clear ice embedded within longitudinally foliated ice of the englacial diffused facies, which could be traced for long distances across the glacier surface. Debris was commonly derived from a single rock type and was coarse-grained and predominantly angular in shape. The incorporated rock types varied systematically across the glacier in a manner consistent with their pattern of outcrop on the valley walls. This suggests that the debris was initially deposited on the glacier surface in the accumulation area, buried by winter snowfall and transported down-glacier in an englacial position before being brought back to the surface by ablation. The debris bands may therefore represent accumulations of debris on summer melt surfaces or material deposited on to the glacier by individual mass-movement events.

Basal stratified facies — laminated sub-facies (Bs_l)

The most widespread component of the basal stratified facies consisted of repeated laminations of clear and debris-rich ice (Fig. 4). In general, the laminae were flat-lying and sub-parallel to the glacier bed (cf. foliation S_b of Pfeffer (1992)) but they were locally folded. The orientation of the laminae was discordant with that of foliation in overlying Ed-facies ice. The clear ice layers were up to 2 cm thick and were composed of crystals generally less than 0.3 cm in diameter. Locally, however, crystals up to 3 cm in diameter cross-cut the lamination. Such crystals were presumably a product of secondary recrystallization. The debris-rich laminae were up to 0.3 cm thick and were composed of ice crystals up to 0.1 cm in diameter, which were commonly elongated perpendicular to the lamination. Air bubbles were rare within this facies but they could be concentrated along planes parallel to the lamination which lay immediately above the upper surface of debris-rich layers. Debris concentrations, measured on samples composed of several clear and debris-rich laminae, averaged 10.9% by volume, while electrical conductivities averaged 44 μS cm^{-1} (Table 1).

Debris consisted of a sand- and silt-sized matrix, with coarser clasts occasionally protruding from the upper surface of the laminae into overlying clear ice. Such clasts also occurred dispersed within the clear-ice layers and were composed almost entirely of black ortho-amphibolite, which is the immediately underlying bedrock. Debris samples from the Bs_l sub-facies were characteristically polymodal. Gaussian component analysis re-

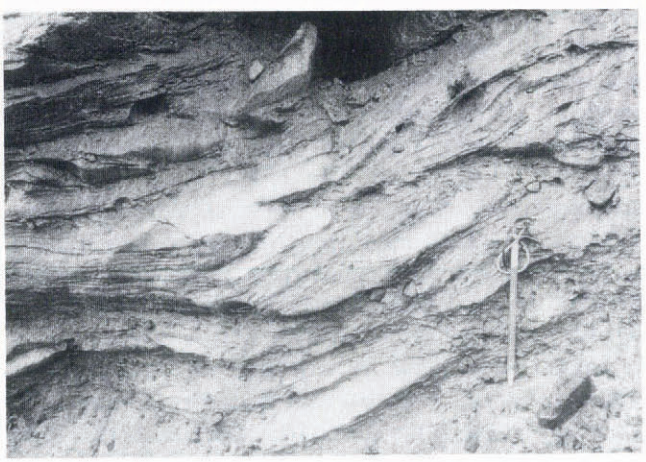

Fig. 4. Basal ice layer at site C, showing pods of Bd-facies ice which occur as intrafolial fold hinges and boudinaged remnants of fold limbs within Bs_l sub-facies ice. Ice axe (85 cm) provides scale.

vealed that four discrete modes occurred repeatedly in samples from this sub-facies (although all four were not present in every sample) (Fig. 3). These modes were centred on 6.5Φ (fine silt), 3Φ (fine sand), −1.5Φ (fine gravel) and −3.5Φ (medium gravel). The fine-sand mode was commonly the dominant one (30–60%), although this was not always the case (Fig. 3b).

It seems probable that these particle-size modes can be interpreted in terms of the processes of comminution which affect debris in the subglacial environment (Haldorsen, 1981). The fine-silt mode would therefore represent the products of glacial abrasion and be composed of debris particles finer than the mineral grains in the parent bedrock. The fine-sand mode would represent the products of crushing and would be composed of particles comparable in size to mineral grains in the bedrock. The two coarser modes would represent the products of bedrock fracture and would be composed of lithic fragments. If this interpretation is correct, then the consistent occurrence of three or four of these modes in ice of the laminated sub-facies suggests that it formed in areas of intimate ice–bed contact, where rock debris was being actively produced and comminuted.

Although four size modes were recognized in samples of debris from the laminated sub-facies, the majority of samples could be described adequately using only the three finer modes. It was therefore possible to recognize two sub-types of debris-size distribution. *Low-level* samples, collected from site B (where basal ice was less than 1.5 m thick) and from the lowest 3.9 m of site D (where basal ice was at least 13 m thick), displayed all four modes. *High-level* samples, collected from higher levels at site D, displayed only the three finer modes. For purposes of comparing the two sets of samples, we combined the two gravel-sized modes of samples with four modes and determined the mean proportions of each group of samples which fell into the gravel sand- and silt-sized modes, respectively. Low-level samples were composed, on average, of 50% gravel, 30% sand and 20% silt, while high-level samples were composed of 25% gravel, 45% sand and 30% silt. The low-level samples were therefore enriched in gravel and depleted in the finer grain-sizes relative to the higher-level samples. The enrichment in gravel resulted from addition of the fourth, very coarse mode, which was absent at higher levels in the sequence.

Whilst the addition of the fourth mode to the low-level samples is obviously a real effect, the depletion in silt- and sand-sized debris need not be so. It could arise simply because the addition of the fourth mode automatically reduced the fraction of the sample assigned to the other modes. To test this hypothesis, we calculated the fraction of the low-level samples which would fall into the three finer modes if the fourth mode were not present. In four out of five cases, the low-level samples still contained less silt than the high-level ones and in three out of five cases they also contained less sand. In no case did they contain less gravel. This suggests that the low-level samples were preferentially depleted in silt and, to a lesser extent sand, relative to the high-level samples. This implies either that the ice from which the low-level samples were derived formed at a time when, or in a place where, debris comminution by crushing and abrasion was less active than it was when the high-level ice was formed, or that the subglacial hydrological conditions when the low-level ice was formed favoured the flushing of comminution products from beneath the glacier. The occurrence of the fourth, coarse mode in the low-level samples suggests that bedrock fracture was particularly active when the ice from which they were collected formed. It is hard to envisage an environment in which bedrock fracture would be enhanced but comminution suppressed, so we favour the suggestion that there was efficient flushing of comminution products when the low-level ice formed.

Basal stratified facies — clear sub-facies (Bs_c)

At elevations of more than 3.9 m above the bed at site D, the basal stratified facies contained much thicker lenses of clear ice than occurred within the laminated sub-facies. These lenses could be decimetres thick and several metres wide and they tended to pinch out laterally within the more pervasive laminated ice. Ice crystals were up to 4 cm in diameter. The bubble content of the ice was low and bubbles were concentrated along high-angle planes, aligned parallel to the local ice-flow direction, which cross-cut the ice layers. These planes are interpreted as incipient fracture surfaces (cf. foliation S_2 of Pfeffer (1992)). Pfeffer argued that this foliation formed in response to transverse lateral extension or longitudinal compression within the propagating front of the 1982–83 surge. Thus, the distribution of these fracture surfaces implies that the Bs_c-facies ice, and therefore the basal-ice sequence at elevations greater than 3.9 m above the bed at site D, was entrained within the glacier prior to the 1982–83 surge. Debris concentrations in this facies averaged 0.4% by volume and electrical conductivities averaged 22.8 $\mu S\,cm^{-1}$ (Table 1). Included debris consisted of scattered coarse clasts and grit particles, dispersed randomly through the ice.

Basal stratified facies — solid sub-facies (Bs_s)

This sub-facies consisted of layers up to 80 cm thick of massive structureless debris with interstitial ice. Occasionally, there were more extensive lenses of clear, debris-free ice within the debris. The layers had undulating boundaries and could, in places, be traced laterally for tens of metres. They ablated more slowly than the laminated ice and, at site D, protruded from the ice surface, splitting the basal ice layer into a series of wedges, each up to several metres thick (Fig. 5). Clasts up to 26 cm in length derived from a variety of lithologies (including the local ortho-amphibolite, greenschist, mica-schist and a quartzite) were recovered from this facies. This clearly differentiates the debris in this facies from that in the Bs_l sub-facies, which was all locally derived. No obvious primary sedimentary structures were observed within the debris of this facies. However, the ice lenses were commonest in the more silt-rich layers, suggesting an origin as segregation ice lenses (cf. Tison and others, 1989). Debris concentrations averaged 36% by volume and electrical conductivities averaged 60.7 $\mu S\,cm^{-1}$ (Table 1).

Size distributions of Bs_s sub-facies debris were

https://doi.org/10.3189/S0022143000007413 Published online by Cambridge University Press

Fig. 5. Basal stratified facies ice at site D, where the sequence is split into wedges by the outcrop of bands of Bs_s sub-facies ice.

polymodal but the modes recognized by Gaussian component analysis were inconsistent between samples and frequently did not correspond with those found in the laminated sub-facies (Fig. 3). Although only four samples were analysed and three different types of composition were observed, these are believed to be representative of the range of debris types found within this facies. Type (a) sediment had three modes but 89% of the sample consisted of coarse-to-medium silt, similar to that found in the Ed facies. Type (b) had three modes and a size distribution very similar to that of high-level Bs_l sub-facies debris. Type (c) had four modes, the most prominent of which consisted of fine-to-medium gravel and of coarse-to-medium sand. Together, these modes comprise over 70% of the size distribution.

Basal diffused facies (Bd)

Enclosed within the basal stratified facies were layers and pods of ice, up to 0.65 m thick and 1.1 m in lateral extent, with physical characteristics indistinguishable from those of Ed-facies ice. On account of its occurrence within the basal stratified ice, this ice is referred to as the *basal* diffused facies. It occurred in two main situations: at site D it cropped out in a well-defined zone immediately above the bed as a breccia, in which individual blocks showed different foliation orientations (Fig. 2); however, at sites B and C, and at higher levels of site D, isolated pods occurred throughout the thickness of the basal ice layer as boudinaged remnants of formerly more extensive layers and as rootless intrafolial fold hinges (Fig. 4). Debris concentrations and electrical conductivities of these pods were very similar to those of the Ed facies (Table 1).

ISOTOPIC COMPOSITION OF THE ICE

Englacial diffused facies and snow

Snow, sampled in the ablation zone, and Ed-facies ice had a relatively wide range of isotopic compositions (Table 2). Values were somewhat heavier than others reported for the St Elias Range (Epstein and Sharp, 1959; MacPherson and Krouse, 1967; West and Krouse, 1972) but they were consistent with the lower elevations at which sampling took place on Variegated Glacier. West and Krouse (1972) suggested that $\delta^{18}O$ decreased with altitude at a rate of 0.4‰ per 100 m on Rusty Glacier, Yukon Territory. They recorded a mean $\delta^{18}O$ value of −22‰ at 2640 m on Hubbard Glacier, which lies immediately to the west of Variegated Glacier. Given these results and the altitude distribution of Variegated Glacier (0–1950 m), a range of composition of −11.40 to −19.30‰ in $\delta^{18}O$ is predicted. This is very close to the observed range for snow and Ed-facies ice (−12.60–−18.75‰).

The δD versus $\delta^{18}O$ relationship for samples of snow and Ed-facies ice is described by the line $\delta D = 6.57(\pm 0.27)\delta^{18}O - 14.97$ ($r^2 = 0.92, DF = 54, p < 0.001$) Separate treatment of snow and Ed-facies samples reveals similar trends. For snow $\delta D = 6.73(\pm 0.33)\delta^{18}O) - 15$ ($r^2 = 0.98$, $DF = 9$, $p < 0.001$), while for Ed-facies ice from the glacier centre line $\delta D = 6.54(\pm 0.73)\delta^{18}O - 15.3$ ($r^2 = 0.8$, $DF = 21$, $p < 0.001$). Allowing for the standard errors on the slope coefficients, the slopes of these lines are lower than the global average value of 8 normally found in samples of precipitation and unaltered glacier ice (Dansgaard, 1964). They are, however, similar to the value of 6.86 determined from monthly mean values of precipitation at Adak (the only Alaskan site for which there are data from the IAEA network). Thus, although we cannot completely rule out the possibility that the empirically determined slopes correspond to the local precipitation slope, it seems likely that both snow and Ed-facies ice have undergone some isotopic fractionation relative to precipitation.

Since co-isotopic analysis suggestes that fractionation may affect both old snow and Ed-facies ice, it seems likely that this occurs from the earliest stages of firnification. At Variegated Glacier, firnification occurs entirely within the wetted zone, in which isotopic fractionation (and lowering of the co-isotopic slope relative to that of precipitation) might result from two main processes: (a) evaporation, which enriches the surface of the snowpack in D and especially ^{18}O, and makes percolating meltwaters derived from the enriched surface layer isotopically heavier than the original snow (Stichler and Herrmann, 1978; Moser and Stichler, 1980; Stichler and others, 1982); and (b) fractionation between snow and percolating meltwater during recrystallization of the snowpack, which results in the enrichment of the snowpack in heavy isotopes, particularly ^{18}O (Arnason, 1969, 1980; Martinec and others, 1977; Moser and Stichler, 1980; Stichler and others, 1982). These processes may have had a particularly marked effect on the co-isotopic characteristics of snow and Ed-facies ice at Variegated Glacier because of the unusually low elevation of its accumulation area and because of the periodic occurrence of Chinook winds which induce strong evaporation from the snowpack. If individual samples of snow and glacier ice display varying degrees of isotopic fractionation relative to precipitation depending upon the environment in which firnification took place, then empirical co-isotopic slopes determined from groups of such samples may be purely statistical artefacts which fall

Table 2. Summary of the stable-isotope composition of ice facies sampled at Variegated Glacier. For basal ice, results are presented for the basal stratified facies as a whole, and also for the individual sub-facies. No data are available for the englacial banded facies

	$\delta^{18}O$ ‰				δD ‰				
Facies	*Max.*	*Min.*	*Mean*	*Std dev.*	*Max.*	*Min.*	*Mean*	*Std dev.*	*Sample size*
Snow	−12.60	−18.75	−15.45	1.88	−100.00	−142.60	−118.87	12.78	11
Englacial diffused	−14.55	−17.70	−16.34	0.87	−109.60	−132.30	−122.12	6.35	23
Basal diffused	−13.50	−15.55	−14.75	0.57	−103.30	−116.20	−111.63	3.93	13
Basal stratified	−13.20	−16.00	−14.28	0.67	−101.40	−118.80	−108.75	4.12	48
Basal stratified laminated	−13.35	−15.75	−14.24	0.59	−101.40	−116.50	−108.87	3.69	33
Basal stratified clear	−13.20	−16.00	−14.46	0.86	−101.60	−118.80	−108.94	5.32	11
Basal stratified solid	−13.35	−15.00	−14.06	0.55	−102.70	−113.30	−107.25	3.33	4

somewhere between the precipitation slope and the theoretical freezing or evaporation slopes (see below).

Basal diffused facies ice

The isotopic composition of Bd-facies ice from sites B–D is slightly heavier than that of snow and Ed-facies ice from the glacier centre line (Table 2) but its co-isotopic characteristics are identical. Samples plot on the line $\delta D = 6.62\ (\pm 0.59)\delta^{18}O - 13.98$ ($r^2 = 0.92$, DF = 11, $p < 0.001$). This result suggests that Ed- and Bd-facies ice have a similar origin, although the slightly heavier isotopic composition of Bd-facies ice may imply a lower mean elevation of formation than that of Ed-facies ice collected on the glacier centre line. Isotopically, Bd-facies ice is distinguishable from the Bs-facies ice by which it is surrounded on the basis of its steeper co-isotopic slope (see below).

Basal stratified facies ice

As a single population, basal stratified ice is isotopically heavier than snow and Ed-facies ice from the glacier centre line but similar in composition to Bd-facies ice found within it (Table 2). Its co-isotopic characteristics are, however, different from those of snow and Ed/Bd-facies ice, since samples plot on lines of lower slope. For the Bs facies as a whole, samples plot on the line $\delta D = 5.81\ (\pm 0.32)\delta^{18}O - 25.87$ ($r^2 = 0.88$, DF = 46, $p < 0.001$). When sub-facies are considered, the Bs_c facies is most similar to Bd-facies ice ($\delta D = 6.09(\pm 0.39)\delta^{18}O - 20.9$; $r^2 = 0.97$, DF = 9; $p < 0.001$), while Bs_l and Bs_s are more dissimilar (Bs_l: $\delta D = 5.77(\pm 0.45)\delta^{18}O - 26.7$; $r^2 = 0.84$, DF = 31, $p < 0.001$; Bs_s: $\delta D = 5.86(\pm 1.07)\delta^{18}O - 24.8$; $r^2 = 0.94$, DF = 2; NS).

GENESIS OF INDIVIDUAL ICE FACIES

Englacial/basal diffused facies

The results presented above clearly establish the distinction between Ed/Bd- and Bs-facies ice. Ed-facies ice comprises the bulk of the glacier and is produced by firnification processes in the accumulation area. On account of the low elevation of Variegated Glacier, these processes take place entirely within the wetted zone. The co-isotopic characteristics of Ed-facies ice thus appear to show evidence of fractionation between ice and percolating meltwater during recrystallization of the snowpack. Debris incorporated in Ed-facies ice is primarily aeolian in origin, though it also includes small quantities of coarse sand, which may be derived from the valley walls. Locally, higher concentrations of valley-wall-derived material occur within the Eb facies. Bd-facies ice is similar to Ed-facies ice in its physical appearance, debris content, electrical conductivity and co-isotopic characteristics, so the two facies probably have a similar origin. The isotopic composition of Bd-facies ice is heavier than that of the Ed facies sampled on the glacier centre line, suggesting formation at lower elevations. The outcrop geometry of Bd-facies ice suggests that it has become tectonically incorporated within the basal ice layer.

Basal stratified facies—laminated sub-facies

Bs_l sub-facies ice is physically, structurally and co-isotopically distinct from overlying Ed-facies ice. The laminae within it are discordant with the foliation in Ed-facies ice and they are defined by variations in debris concentration rather than in bubble content. The overall debris content is much higher and the bubble content much lower than in the Ed facies. These characteristics suggest either that the BS_l sub-facies ice has been accreted

https://doi.org/10.3189/S0022143000007413 Published online by Cambridge University Press

on to the base of the glacier by processes quite different to those involved in the formation of Ed-facies ice, or that it has suffered an extreme degree of metamorphism as a result of deformation in the shear zone at the base of the glacier. Whilst there is no doubt that the basal ice layer has been strongly deformed (see below), the extremely sharp nature of the boundary between Ed and Bs_l sub-facies ice leads us to believe that basal accretion has taken place.

The textural characteristics of Bs_l sub-facies debris suggest that it was subglacially derived and entrained in an environment in which bedrock erosion and debris comminution were active. This probably implies a rigid substrate. The lithology of the debris suggests an origin no more than 3 km up-glacier from the sample sites. The contrast in debris character between high- and low-level samples suggests temporal variations in the intensity of bedrock fracture and in the efficiency of fluvial flushing of fine-grained debris within the environment in which this facies was formed. Observations made during the 1982–83 surge suggest that these variations may have been associated with the active and quiescent phases of the surge cycle.

The 1982–83 surge was apparently linked to a change from channelized subglacial drainage during quiescence to distributed subglacial drainage (Kamb and others, 1985; Kamb, 1987), which would have given meltwaters access to a large proportion of the glacier bed. Extremely large quantities of suspended sediment were removed from the glacier during and immediately after the surge (Humphrey, 1985; Sharp, 1988), suggesting that fluvial flushing of comminution products was particularly effective under these conditions. The absence of comminution products from ice which was in close proximity to the bed immediately after the surge suggests that this ice formed and/or interacted with the glacier bed during the surge, when this flushing took place. The presence of comminution products in ice at higher levels above the bed suggests that this ice formed under conditions when debris flushing was less efficient (e.g. meltwaters were confined to a few large subglacial channels) and that it did not interact with the bed during the surge. The observation that Pfeffer's (1992) S_2 surge-induced foliation is present in layers of Bs_c sub-facies ice contained within high-level Bs_l ice confirms that this ice was in existence prior to the 1982–83 surge. Although this ice could have formed during a previous surge, the characteristics of the debris entrained within it suggest that it is more likely to have formed during the quiescent phase of a surge cycle.

The presence of relatively large quantities of medium gravel in the low-level ice suggests that bedrock fracture was an active process when this ice formed. This might be expected under surge conditions, when subglacial water pressures were high (Kamb and others, 1985) and subglacial cavitation was presumably extensive. Such conditions significantly weaken rock on the lee side of bedrock bumps (Boulton, 1974; Röthlisberger and Iken, 1981). Fracture and removal of eroded bedrock are facilitated by fluctuations in the water pressure in leeside cavities (Iverson, 1991). High rates of frictional melting at the glacier bed (associated with high basal shear stresses and large sliding velocities) also favour fracture by inducing unusually high contact forces between entrained particles and the bed (Hallet, 1979).

Laminated ice similar in appearance to the Bs_l sub-facies ice at Variegated Glacier is widespread at the base of glaciers in the western European Alps (Hubbard, 1992), where its formation has been linked to regelation as ice flows over bedrock of irregular geometry (Hubbard and Sharp, 1993). In this model, it is argued that laminated ice forms by refreezing of meltwaters on the downstream side of bumps. Gas and debris (particularly the finer grain-sizes) are rejected from the ice during the initial stages of refreezing (Hubbard, 1991), accounting for the low bubble and debris content of the clear-ice layers. Both debris and air bubbles may, however, be entrapped within the ice during the final stages of freezing, when the residual water becomes supersaturated with respect to dissolved gases, bubble nucleation occurs and the removal of gas from solution raises the freezing point, so that the rate of freezing increases (cf. Rowell and Dillon, 1972). This mechanism can account for the observed association of debris laminae and bubble planes in this facies. Partial melting of debris laminae on the upstream side of bumps of lower amplitude located further downstream may concentrate debris at the ice/bed interface and increase the local debris concentration. Internal melting within the basal ice could have a similar effect (Lliboutry, 1993).

Co-isotopic analyses of BS_l sub-facies ice help to test this hypothesis, because it has been demonstrated that isotopic fractionation during the refreezing of meltwaters usually produces ice samples which plot on a δD versus δ^{18}O diagram with a slope lower than that on which source waters plot (Jouzel and Souchez, 1982; Souchez and Jouzel, 1984). When freezing occurs under closed-system conditions (as in regelation, for instance), this slope (S) is given by:

$$S = \frac{(\frac{\alpha-1}{\beta-1})((1000 + \delta_i \mathrm{D})}{(1000 + \delta_i {}^{18}\mathrm{O})} \quad (1)$$

where α and β are the equilibrium fractionation coefficients for D and ^{18}O, respectively (1.0212 and 1.00291; Lehmann and Siegenthaler, 1991), and δ_i refers to the isotopic composition of the initial (source) liquid (Jouzel and Souchez, 1982). For open-system freezing, in which the composition of the water input to the reservoir during freezing is not significantly different from that of the initial liquid, the slope is given by:

$$S = \frac{(\alpha((\alpha - 1)(1000 + \delta_i \mathrm{D})))}{(\beta((\beta - 1)(1000 + \delta_i^{18}\mathrm{O})))} \quad (2)$$

(Souchez and Jouzel, 1984). On these slopes, samples which plot at the heavy end of the isotopic spectrum form during the early stages of freezing, whereas those which plot at the light end form during the final stages of freezing. For the case of closed-system freezing, the mean isotopic composition of the solid formed at each stage of the freezing process is given by:

$$\delta_s = 10(1000 + \delta_i)((1.1 - K)^{\alpha} - (1 - K)^{\alpha}) - 1000 \quad (3)$$

where δ_s is the isotopic composition of the solid formed and K is the fraction of the liquid reservoir that has frozen (Jouzel and Souchez, 1982).

In evaluating the origin of the Bs_l sub-facies, it is useful to consider whether or not the empirically determined co-isotopic slope for this sub-facies coincides with that predicted using either of the above models. Some caution is, however, necessary in adopting this approach. In previous work, it has been argued that the isotopic composition of the initial liquid can be defined by the point of intersection of the local precipitation slope and the empirically determined slope for basal ice facies (Jouzel and Souchez, 1982). This makes two assumptions which are not necessarily valid: (i) that all samples of basal ice analysed are derived from initial liquids of identical composition, and (ii) that these initial liquids lie on the local precipitation slope. The first assumption ignores the range of isotopic compositions which characterizes waters in the glacial environment and assumes that the empirically determined basal ice slope is equivalent to the physically meaningful theoretical freezing slope. If, in reality, basal ice forms from a range of initial liquids, the empirically determined slope may be no more than a statistical artifact. The second assumption ignores the possibility that melting of pre-existing basal ice can provide the initial liquid for later generations of such ice and that such initial liquids may not lie on the precipitation slope.

We therefore make the more realistic assumption that basal ice could potentially form from any initial liquid within the range of compositions measured at Variegated Glacier. Taking initial liquids at the light and heavy extremes of the waters sampled (−142.60‰ δD and −18.75‰ δ^{18}O, and −100.00‰ δD and −12.60‰ δ^{18}O, respectively), the predicted freezing slopes are 6.37 and 6.64 (closed system; Equation (1)), and 6.48 and 6.76 (open system; Equation (2)), respectively. These are all steeper than the empirically determined slope for the Bs_l sub-facies (5.77 ± 0.45). Although the fact that the empirical slope is gentler than the local precipitation slope is consistent with the suggestion that the Bs_l ice formed by the refreezing of meltwaters, the poor correspondence between the theoretical and empirical slopes suggests either that the latter is a statistical artefact (resulting from basal ice forming from a variety of initial liquids) or that the isotopic composition of the Bs_l sub-facies ice has undergone modification subsequent to its formation.

Let us first consider the possibility that basal ice forms from a range of initial liquids. Taking, as examples, initial liquids at the light and heavy extremes of measured values of snow and Ed-facies ice, and plotting the theoretical freezing slopes derived from these on a co-isotopic (δD versus δ^{18}O) diagram, it is possible to define an envelope within which samples of basal ice should plot (Fig. 6). For the case of closed-system freezing, it is possible to use Equations (1) and (3) to define a grid within this envelope. In this grid, the sub-horizontal lines represent freezing slopes derived from different initial liquids. The sub-vertical lines link points on different freezing slopes corresponding to equivalent frozen fractions of their respective initial liquids (Fig. 6). The position within the grid at which an individual sample plots is determined by (a) the composition of the initial liquid, and (b) the frozen fraction represented by the

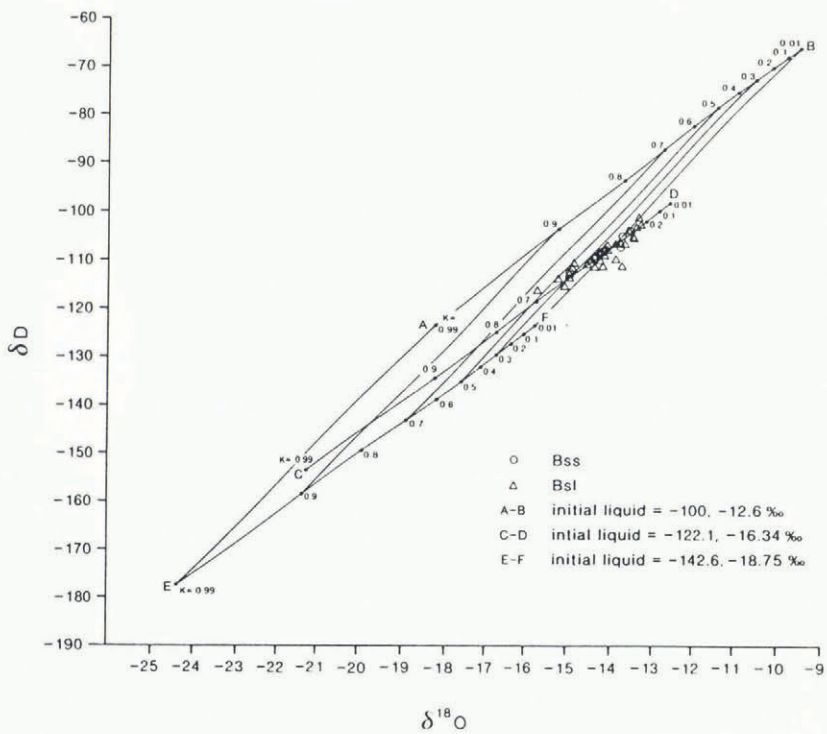

Fig. 6. Co-isotopic diagram, showing the envelope within which should lie samples of basal ice formed by the freezing meltwaters within the range of isotopic compositions defined by samples of snow and Ed-facies ice. Sub-horizontal lines are theoretical freezing slopes for different initial liquids, and span the range of compositions produced by freezing of different initial liquids. Crosses on these lines define the predicted isotopic composition of different frozen fractions. Sub-vertical lines link points corresponding to equivalent frozen fractions. Freezing slopes are plotted for initial liquids at the light and heavy extremes of samples of snow and Ed-facies ice (see text), and with a composition equivalent to the mean of Ed-facies ice (−122.12‰δD, −16.34‰δ^{18}O). Circles and triangles represent samples of Bs_s and Bs_l sub-facies ice, respectively.

https://doi.org/10.3189/S0022143000007413 Published online by Cambridge University Press

sample. Some of the samples of Bs_l sub-facies ice plot outside and to the right of this grid, implying that they formed from initial liquids slightly enriched in ^{18}O relative to those used to define the envelope. However, all of the samples plot close to the freezing slope for an initial liquid comparable in composition to or slightly ligher than the mean of Ed-facies ice on the glacier centre line (−122.1 and −16.34‰), and within the range of isotopic compositions which could be produced by freezing such a liquid (frozen fractions of 0.2–0.7). This suggests (i) that, if Bs_l sub-facies ice was formed by refreezing of meltwaters, refreezing actually took place under open-system conditions (because K values are <1), and (ii) that the waters involved in refreezing were isotopically more homogeneous than the range of possible initial liquids at Variegated Glacier.

Open-system freezing would be expected if regelation was accompanied by net basal melting due to geothermal heating or sliding friction. Net melting would result in a continuous influx to the freezing environment of water derived from Ed-facies ice, ensuring that the isotopic composition of the initial liquid remained close to that of Ed-facies ice. Initial liquids lighter in composition than the mean of Ed-facies ice could be produced by isotopic fractionation accompanying recrystallization either in the basal shear zone of the glacier (see below) or during firnification.

One problem in applying this model to the basal ice sequences at Variegated Glacier lies in the difficulty of explaining the large thicknesses of Bs_l ice observed. Theoretical considerations and simple modelling (Lliboutry, 1993; Hubbard and Sharp, 1993) suggest that ice layers produced by this mechanism should not exceed a few decimetres in thickness (or less if there is net basal melting). Whilst such thicknesses are consistent with those observed at site A and possibly site B, they are much less than observed at sites C and D. Two mechanisms might explain this discrepancy: (i) the basal ice was formed by net basal adfreezing rather than by regelation, or (ii) the basal ice layer was thickened significantly by tectonic processes. Net basal adfreezing seems unlikely in the case of Variegated Glacier, because it is known to have a temperate thermal regime, and because it probably experiences high rates of net basal melting during surges which would have the effect of thinning rather than accreting a basal ice layer. The role played by tectonic processes is discussed below.

As an alternative to the regelation model discussed above, it is possible that the co-isotopic characteristics of Bs_l sub-facies ice result from recrystallization, partial melting and loss of isotopically light meltwater from basal ice resulting from high stresses and strain rates close to the glacier bed, particularly under surge conditions. However, three factors lead us to believe that this is probably not the case. First, Bd-facies ice enclosed within Bs_l sub-facies ice does not appear to have had its co-isotopic slope modified by such processes. Secondly, such processes do not provide a means of entraining the high debris content of Bs_l sub-facies ice. Thirdly, only a small number of samples of basal ice seem to have formed by refreezing of isotopically light meltwaters such as would have been squeezed from basal ice by these processes. We therefore favour the idea that the Bs_l sub-facies ice formed by regelation in association with net basal melting, although we cannot totally rule out the possibility that the isotopic composition of the ice has been modified by fractionation accompanying recrystallization. The sub-horizontal and planar nature of the lamination within this facies may, however, be attributable to rotation of fabric elements into the plane of shear.

Basal stratified facies — clear sub-facies

The occurrence of S_2 foliation within Bs_c sub-facies ice suggests that it formed prior to the 1982–83 surge, and its outcrop within Bs_l sub-facies ice which contains comminution products suggests that it may well have formed during the quiescent phase of a surge cycle. Again, the question arises as to whether it was accreted on to the glacier sole by the refreezing of meltwaters, or whether it represents a metamorphosed form of Ed-facies ice. The low debris content and electrical conductivity of the ice are comparable to those of the Ed and Bd facies but the bubble content is much lower. The co-isotopic slope of Bs_c sub-facies ice (6.09 ± 0.39) is intermediate between those of Ed and Bs_l ice. Whilst it is difficult to draw unequivocal conclusions about the origin of the Bs_c sub-facies on the basis of these data, the similarities to Ed-facies ice and the intermediate isotopic characteristics suggest that an origin as metamorphosed Ed- or Bd-facies ice may be more likely than formation by basal freezing. If this view is correct, the low bubble content of the ice would be explained as a result of the removal of gases in solution by percolating meltwater (cf. Berner and others, 1978), while the intermediate co-isotopic slope would be linked to the processes of recrystallization, partial melting and meltwater squeezing described above. This then suggests that Bs_c sub-facies ice is identical in origin to Bd-facies ice but that its physical appearance and co-isotopic characteristics have been modified as a result of it experiencing a much higher degree of metamorphism.

Basal stratified solid sub-facies ice

The character of solid sub-facies debris suggests that it consists of sediments which were accreted en masse (rather than particle-by-particle) on to the base of the glacier (cf. Lawson, 1979). It is therefore likely that this sub-facies formed where the glacier bed consisted of unconsolidated sediments, while the Bs_l sub-facies formed where it consisted of rigid bedrock. The co-isotopic characteristics of the Bs_s sub-facies are indistinguishable from those of the Bs_l sub-facies, suggesting that the ice formed by open-system freezing, with metamorphic effects possibly superimposed. The size characteristics of the sediments suggest considerable variation in the character of the source sediments, reflecting the range of transport and depositional processes active in the subglacial environment. Type (b) debris, which contains a wide range of particle sizes, probably originated as subglacial (perhaps lodgement) till, which was observed in the proglacial area a short distance from site D. Types (a) and (c) show a greater degree of sorting and are probably fluvial or lacustrine in origin. Type (c) contains very little silt- and clay-sized material, and has a size distribution characteristic of glaciofluvial gravels. Type (a) consists

primarily of silt and represents a lower-energy depositional environment. It is significant that types (a) and (c) were most commonly observed at site D, which is immediately adjacent to one of the main meltwater streams draining the glacier. This suggests that the sediments may have been transported and deposited by this stream prior to being entrained by the glacier. Type (c) sediments were probably deposited within the stream channel or on a bar within it, while type (a) sediments were deposited in a slack-water environment. Long-distance debris transport by glacial meltwaters can account for the occurrence of exotic lithologies in the debris of this facies.

INFLUENCE OF TECTONIC PROCESSES ON THE GEOMETRY OF THE BASAL ICE LAYER

In the above discussion of the genesis of individual ice facies within the basal ice layer of Variegated Glacier, it was noted that there was a problem in explaining the observed thickness of the ice layer at sites B, C and D in terms of an origin by regelation. Thickening of the basal ice layer by tectonic processes can help to resolve this problem, so we now consider the evidence for whether and how this occurred. It should be remembered that the exposures of basal ice lie within the area of the glacier affected by intense longitudinal compression associated with the down-glacier propagation of the 1982–83 surge front (Raymond and others, 1987). Within an equivalent area close to the glacier centre line, the horizontal shortening during the surge decreased up-glacier from 53% to less than 10% over a distance of about 800 m (approximately the distance from site D to site A) (Pfeffer, 1992). This shortening was accommodated primarily by vertical rather than transverse extension (Raymond and others, 1987; Sharp and others, 1988; Pfeffer, 1992).

At sites A–C, where the basal ice was less than 3–4 m thick, it formed a discrete layer which underlay Ed-facies ice, although there were pods of Bd-facies ice within it. These sites revealed a sequence of increasingly intense deformation consistent with the down-glacier increase in horizontal shortening referred to above (Fig. 7). The structures produced by this deformation were confined to the basal ice layer and immediately overlying Ed-facies ice. The style of deformation suggests that the basal ice layer at these sites acted as a ductile, high-strain layer during the surge. In a down-glacier direction, the style of folding changed from (i) rooted, upright folds to (ii) rooted, overturned to recumbent folds, the overturned limbs of which were cut by thrust faults along which displacements of a few decimetres had occured (Fig. 8), to rootless recumbent folds the overturned limbs of which were cut by flat-lying thrust faults which split the basal ice layer into a stacked sequence of thin (< 0.8 m) glide nappes, and the upper limbs and fold hinges of which were boudinaged (with Bd-facies ice behaving as the more competent layer) (Fig. 4).

This fold sequence probably represents (i) the initial buckling response of adjacent layers of contrasting competence (in which the debris-rich basal ice appears to have behaved as the less-competent layer) to imposed longitudinal compression; (ii) superimposition of shear strain on the growing upright folds, and (iii) the onset of heterogeneous deformation within the basal ice layer as overturned fold limbs experienced shear thinning and rotation into parallelism with the plane of shear. Down-glacier thickening of the basal ice layer from a few decimetres to 3–4 m was accomplished by a combination of continuous deformation and nappe over-riding, the latter becoming more important in a down-glacier direction. Ed-facies ice was incorporated into the basal ice layer (to form Bd-facies ice) by two principal processes: (a) as synform remnants beneath the over-

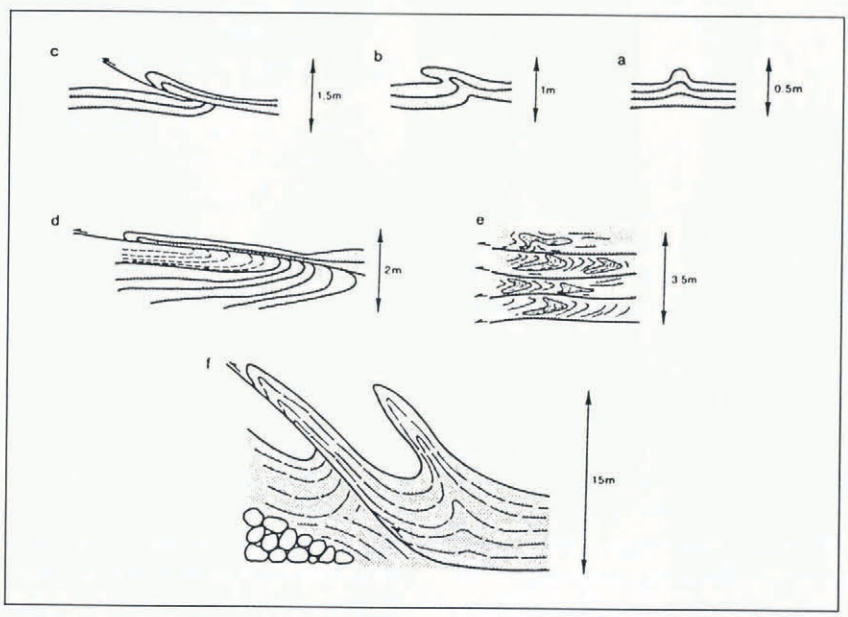

Fig. 7. Schematic diagram to show down-glacier changes in the geometry of the basal ice layer at Variegated Glacier and in the style of deformational structures associated with it. (a) describes the situation at site A; (b) site B; (e) site C and (f) site D, (while (c) and (d) are hypothetical intermediate stages). Stippling defines Bs-facies ice. Unstippled areas consist of Ed or Bd facies.

https://doi.org/10.3189/S0022143000007413 Published online by Cambridge University Press

Fig. 8. Rooted overturned folds in Bs_l sub-facies ice at site B. Ice hammer (30 cm) provides scale.

turned limbs of rooted recumbent folds, and (b) entrapment beneath over-riding glide nappes (Fig. 7).

At site D, the thickness of the contiguous basal ice layer increased to around 13 m, although approximately 20% of the ice within it was Bd-facies ice. This ice was concentrated in a layer 3 m thick at the base of the sequence (Figs 2 and 7). In addition, debris bands composed of Bs_l sub-facies ice cropped out at elevations up to 50 m above the bed and were separated from each other and from the contiguous basal ice layer by layers of Ed-facies ice up to 10 m thick (Fig. 7). Three main processes, all of which were observed to occur during the 1982–83 surge, seem to account for the geometry of the basal ice layer at this site:

(i) Apron over-riding (Shaw, 1977; Evans, 1989). As the glacier advanced across the outwash deposited by the meltwater stream in June 1983, blocks of Ed-facies ice spalled from higher levels on the glacier surface collected at the base of the advancing ice front and were over-ridden by it. They were incorporated into the basal ice layer as a breccia composed of large flattened blocks of Bd-facies ice, in which foliation orientations varied from block to block.

(ii) Intrusion of ductile basal ice into the core of large frontal anticlines which grew at the distal limit of the down-glacier-propagating sole thrust over which the surging part of the glacier was moving (Sharp and others, 1988). Rotation of this basal ice (mainly Bs_l sub-facies) as the anticlines were overturned produced up-glacier-dipping debris bands, which have been exposed at the glacier surface as the cores of the anticlines have been unroofed by post-surge ablation.

(iii) Upward ramping of imbricate thrust faults from the basal décollement through the overturned limbs of the growing anticlines. These thrust faults rise more steeply from the bed than those which occur solely within the basal ice layer. Basal ice attached to the hanging wall of these thrusts was emplaced to relatively high elevations above Ed-facies ice along them. This process seems to have been particularly important in emplacing Bs_s sub-facies ice within the basal ice layer.

DISCUSSION AND CONCLUSIONS

This study has identified four sets of processes which contributed to the formation of the ice facies that comprise the basal ice layer of Variegated Glacier. The predominant sub-facies (Bs_l and Bs_s) seem to have formed by open-system freezing of subglacial meltwaters, Bs_l over rigid substrates which were being actively eroded and Bs_s over unconsolidated substrates which were permeable to both ice and water. Bd facies seems to be Ed-facies ice which was incorporated within the basal ice layer by apron over-riding and tectonic processes such as recumbent folding and nappe over-riding. Bs_c sub-facies ice appears to be a highly metamorphosed form of Bd-facies ice, from which the air bubbles were removed by dissolution of gases in percolating meltwaters. The physical and co-isotopic characteristics of all of the basal-ice facies may have been modified by recrystallization, partial melting and squeezing out of water arising from intense deformation within the basal shear zone of the glacier.

The characteristics of the debris contained within the Bs_l sub-facies suggest that the majority of the basal ice layer formed during the surge phase of a surge cycle, when bedrock fracture and meltwater flushing of comminution products were particularly effective. High rates of net basal melting during the 1982–83 surge may have helped to destroy or rework any basal ice layer formed during quiesence. At site D, however, structural evidence and the grain-size characteristics of debris from the Bs_l sub-facies suggest that the quiescent-phase basal ice layer was preserved above that formed during the surge. Site D is located close to the position of maximum horizontal shortening recorded during the surge, so preservation of the quiescent-phase basal ice layer suggests that tectonically induced thickening of the basal ice layer more than offset net basal melting during the surge in this location. Since this area was only briefly incorporated into the fully surging part of the glacier in 1983, total basal melting during the surge may well have been quite small, while the tectonically induced thickening was about 100%. Within the quiescent-phase basal ice layer, Bs_c sub-facies ice largely replaced Bd-facies ice, supporting the notion that Bd ice may evolve into Bs_c ice as its age and degree of deformation increase.

The thickness of the basal ice layer increased down-glacier in a manner consistent with the degree of horizontal shortening experienced during the 1982–83 surge. This thickening appears to be largely attributable to tectonic processes and was associated with a down-glacier change in style of deformation. At up-glacier sites, where horizontal shortening was small, folding was confined to the basal ice layer and immediately overlying ice. Folds were upright and rooted and there was minimal thrust-faulting. Further down-glacier, folds became overturned, more strongly attenuated and rootless, and thrust-faulting increased. Nappe over-riding became an important means of thickening the basal ice layer. At site D, deformation involved a considerable thickness of Ed-facies ice above the basal ice layer. Basal ice was emplaced within Ed-facies ice by large-scale recumbent folding and thrust-faulting, both of which resulted from deformation associated with the down-glacier propagation of the basal

sole thrust over which the surging part of the glacier was moving. Where the surge resulted in glacier advance, Bd-facies ice was added to the base of the glacier by apron over-riding. We stress that it seems possible to account for much of the observed thickness of the basal ice layer by reference to the effects of tectonic processes. Intense longitudinal compression is characteristic of the propagation of glacier surges into the terminal regions of glaciers and it is largely accommodated by vertical extension. This creates optimum conditions for thickening a basal ice layer, which at the onset of the surge may have been no more than a few decimetres thick.

Three main points of geomorphological interest emerge from this study. First, tectonic processes which occur during the surge phase of the cycle are largely responsible for the formation of thick basal-ice sequences in surge-type glaciers. The existence of such basal ice layers is a prerequisite for *supraglacial* sedimentation and resedimentation of *subglacially derived* debris, and for the formation of "multiple-till" sequences (Boulton, 1972). It also contributes to the formation of ice-cored moraines and, eventually, "dead-ice" terrain. The notion that such basal ice layers can form only near the margins of sub-polar glaciers where large-scale refreezing takes place, and that the existence in the landscape of their geomorphic and sedimentological products provide evidence for the former existence of glaciers of sub-polar thermal regime is clearly contradicted by the results of this study.

Secondly, the processes of apron entrainment, which have hitherto been associated with the margins of polar glaciers (Shaw, 1977; Evans, 1989), have now been observed at a wholly temperate glacier. In polar regions, apron over-riding is possible because rates of ablation of spalled ice blocks are extremely low. In temperate regions, rates of ablation are much higher and spalled blocks are only likely to survive to be over-ridden if rates of glacier advance are unusually high, as they may be during glacier surges.

Thirdly, the existence of two distinct populations of debris in Bs_l sub-facies ice suggests that the balance of erosion processes active at the glacier bed may change over a surge cycle. Bedrock fracture seems to be particularly effective under surge conditions, as does meltwater flushing of fine-grained sediment. Production of fines by abrasion of larger clasts and intact bedrock may also be effective during surges, particularly since effective flushing of the ice–bed interface may maintain the clean contact necessary for effective abrasion.

ACKNOWLEDGEMENTS

Field work was funded by grants from the Royal Society, the Nuffield Foundation and Christ Church, Oxford. B.H. and W.J.L. acknowledge the receipt of U.K. NERC studentships (GT4/88/GS/22 and GT4/85/GS/24). J. C. Gemmell assisted with the field work, and C. F. Raymond made it possible for us to work at Variegated Glacier. P. Barrett suggested and facilitated the application of Gaussian components analysis. We thank R. A. Souchez, R. D. Lorrain, J.-L. Tison, G. de Q. Robin, I. C. Willis, G. H. Brown and two anonymous referees for their constructive criticisms of earlier drafts. Permission to work at Variegated Glacier was granted by the U.S. National Park Service (Wrangell–St Elias National Park) and Forest Service (Tongass National Forest). Logistic support was provided by M. Ivers of Gulf Air, Yakutat. The paper was written while M.J.S. was on sabattical leave at the University of Alberta. M.J.S. acknowledges receipt of a Royal Society U.K./NSERC scientific exchange award.

REFERENCES

Arnason, B. 1969. The exchange of hydrogen isotopes between ice and water in temperate glaciers. *Earth Planet. Sci. Lett.*, **6**(6), 423–430.

Arnason, B. 1980. Ice and snow hydrology. *In* Gat, J. R., *ed. Stable isotope hydrology: deuterium and oxygen 18 in the water cycle*. Vienna, International Atomic Energy Authority, 143–175. (Technical Report 210.)

Berner, W., B. Stauffer and H. Oeschger. 1978. Dynamic glacier flow model and the production of internal meltwater. *Z. Gletscherkd. Glazialgeol.*, **13**(1/2), 1977, 209–217.

Bindschadler, R., W. D. Harrison, C. F. Raymond and C. Gantet. 1976. Thermal regime of a surge-type glacier. *J. Glaciol.*, **16**(74), 251–259.

Bindschadler, R., W. D. Harrison, C. F. Raymond and R. Crosson. 1977. Geometry and dynamics of a surge-type glacier. *J. Glaciol.*, **18**(79), 181–194.

Boulton, G. S. 1972. Modern Arctic glaciers as depositional models for former ice sheets. *J. Geol. Soc. London*, **128**(4), 361–393.

Boulton, G. S. 1974. Processes and patterns of glacial erosion. *In* Coates, D. R., *ed. Glacial geomorphology*. Binghamton, State University of New York, 41–87.

Clapperton, C. M. 1975. The debris content of surging glaciers in Svalbard and Iceland. *J. Glaciol.*, **14**(72), 395–406.

Dansgaard, W. 1964. Stable isotopes in precipitation. *Tellus*, **16**(4), 436–468.

Epstein, S. and R. P. Sharp. 1959. Oxygen-isotope variations in the Malaspina and Saskatchewan glaciers. *J. Geol.*, **67**(1), 88–102.

Evans, D. J. A. 1989. Apron entrainment at the margins of sub-polar glaciers, north-west Ellesmere Island, Canadian High Arctic. *J. Glaciol.*, **35**(121), 317–324.

Frost, B. R. 1976. Reconnaissance geology along Variegated Glacier, St. Elias Mountains. *Short Notes on Alaskan Geology*, 1976, 1–4.

Haldorsen, S. 1981. Grain-size distribution of subglacial till and its relation to glacial crushing and abrasion. *Boreas*, **10**(1), 91–105.

Hallet, B. 1979. A theoretical model of glacial abrasion. *J. Glaciol.*, **23**(89), 39–50.

Hubbard, B. 1991. Freezing-rate effects on the physical characteristics of basal ice formed by net adfreezing. *J. Glaciol.*, **37**(127), 339–347.

Hubbard, B. 1992. Basal ice facies and their formation in the western Alps. (Ph.D. thesis, University of Cambridge.)

Hubbard, B. and M. Sharp. 1993. Weertman regelation, multiple refreezing events and the isotopic evolution of the basal ice layer. *J. Glaciol.*, **39**(132), 275–291.

Humphrey, N. F. 1985. Suspended sediment discharge during the pre-surge and surge phases of motion, Variegated Glacier. *Ice* 78/79, 18.

Iverson, N. R. 1991. Potential effects of subglacial water-pressure fluctuations on quarrying. *J. Glaciol.*, **37**(125), 27–36.

Jouzel, J. and R. A. Souchez. 1982. Melting-refreezing at the glacier sole and the isotopic composition of the ice. *J. Glaciol.*, **28**(98), 35–42.

Kamb, B. 1987. Glacier surge mechanism based on linked cavity configuration of the basal water conduit system. *J. Geophys. Res.*, **92**(B9), 9083–9100.

Kamb, W. B. *and 7 others*. 1985. Glacier surge mechanism: 1982–1983 surge of Variegated Glacier, Alaska. *Science*, **227**(4686), 469–479.

Lawson, D. E. 1979. Sedimentological analysis of the western terminus region of the Matanuska Glacier, Alaska. *CRREL Rep.* 79–9.

Lawson, W., M. Sharp and M. J. Hambrey. In press. Structural assemblage evolution in a cyclic deformation regime: results from Variegated Glacier, Alaska. *J. Struct. Geol*

Lehmann, M. and U. Siegenthaler. 1991. Equilibrium oxygen- and hydrogen-isotope fractionation between ice and water. *J. Glaciol.*, **37**(125), 23–26.

Lliboutry, L. 1993. Internal melting and ice accretion at the bottom of temperate glaciers. *J. Glaciol.*, **39**(131), 50–64.

MacPherson, D. S. and H. R. Krouse. 1967. O^{18}/O^{16} ratios in snow and ice of the Hubbard and Kaskawulsh glaciers. *In* Stout, G. E., *ed. Isotope techniques in the hydrologic cycle.* Washington, DC, American Geophysical Union, 180–194. (Geophysical Monograph 11.)

Martinec, J., H. Moser, M. de Quervain, W. Rauert and W. Stichler. 1977. Assessment of processes in the snowpack by parallel deuterium, tritium and oxygen-18 sampling. *International Association of Hydrological Sciences Publication* 118 (Symposium at Grenoble 1975 — *Isotopes and Impurities in Snow and Ice*), 220–231.

Moser, H. and W. Stichler. 1980. Environmental isotopes in ice and snow. *In* Fritz, P. and J. C. Fontes, *eds. Handbook of environmental isotope geochemistry. Vol. 1.* New York, Elsevier, 141–171.

Pfeffer, W. T. 1992. Stress-induced foliation in the terminus of Variegated Glacier, Alaska, U.S.A., formed during the 1982–83 surge. *J. Glaciol.*, **38**(129), 213–222.

Post, A. 1969. Distribution of surging glaciers in western North America. *J. Glaciol.*, **8**(53), 229–240.

Raymond, C. F. 1987. How do glaciers surge? A review. *J. Geophys. Res.*, **92**(B9), 9121–9134.

Raymond, C. F. and W. D. Harrison. 1988. Evolution of Variegated Glacier, U.S.A., prior to its surge. *J. Glaciol.*, **34**(117), 154–169.

Raymond, C. F., T. Jóhannesson, T. Pfeffer and M. Sharp. 1987. Propagation of a glacier surge into stagnant ice. *J. Geophys. Res.*, **92**(B9), 9037–9049,

Röthlisberger, H. and A. Iken. 1981. Plucking as an effect of water-pressure variations at the glacier bed. *Ann. Glaciol.*, **2**, 57–62.

Rowell, D. L. and P. J. Dillon. 1972. Migration and aggregation of Na and Ca clays by the freezing of dispersed and flocculated suspensions. *J. Soil Sci.*, **23**(4), 442–447.

Sharp, M. 1985a. "Crevasse-fill" ridges — a landform type characteristic of surging glaciers? *Geogr. Ann.*, **67A**(3–4), 213–220.

Sharp, M. 1985b. Sedimentation and stratigraphy at Eyjabakkajökull — an Icelandic surging glacier. *Quat. Res.*, **24**(3), 268–284.

Sharp, M. 1988. Surging glaciers: geomorphic effects. *Progress in Physical Geography*, **12**(4), 533–559.

Sharp, M., W. Lawson and R. S. Anderson. 1988. Tectonic processes in a surge-type glacier. *J. Struct. Geol.*, **10**(5), 499–515.

Shaw, J. 1977. Till body morphology and structure related to glacier flow. *Boreas*, **6**(2), 189–201.

Sheridan, M. F., K. Wohletz and J. Dehn. 1987. Discrimination of grain-size subpopulations in pyroclastic deposits. *Geology*, **15**, 367–370.

Souchez, R. A. and J. Jouzel. 1984. On the isotopic composition in δD and δ^{18}O of water and ice during freezing. *J. Glaciol.*, **30**(106), 369–372.

Stichler, W. and A. Herrmann. 1978. Variations of isotopes in snow covers as input of temperate glaciers. *Z. Gletscherkd. Glazialgeol.*, **13**, 1977, 181–191.

Stichler, W., D. Baker, H. Oerter and P. Trimborn. 1983. Core drilling on Vernagtferner (Oetztal Alps, Austria) in 1979: deuterium and oxygen-18 contents. *Z. Gletscherkd. Glazialgeol.*, **18**(1), 1982, 23–35.

Tarr, R. S. and L. Martin. 1914. *Alaskan glacier studies.* Washington, DC, National Geographic Society.

Tison, J.-L., R. Souchez and R. Lorrain. 1989. On the incorporation of unconsolidated sediments in basal ice: present-day examples. *Z. Geomorphol. Suppl.*, **72**, 173–183.

West, K. E. and H. R. Krouse. 1972. Abundances of isotopic species of water in the St. Elias Mountains. *Icef. Ranges Res. Proj. Sci. Results*, **3**, 117–130.

The accuracy of references in this text and in this list is the responsibility of the authors, to whom queries should be addressed.

MS received 18 October 1991 and in revised form 5 November 1993